TECHNICAL ARTICLE

Phase Formation and Diffusivity in the Ternary Cu-Zn-In System

Tomasz Czeppe (iD), *Anna Sypien, Anna Wierzbicka-Miernik, Grzegorz Garzeł, and Marek Kopyto*

Formation of the phases in Cu-Zn-In system was investigated by means of diffusion multiples annealed in isothermal conditions. The annealing of three different configurations of joints was performed at increasing temperatures (130, 350, 450 °C): below and above melting temperature of In and above Zn melting temperature. It was found that In revealed the ability for the preferential diffusion in Zn along the grain boundaries, forming the eutectic phase. In all applied temperatures, pure Cu was the barrier for the diffusion of In, while the diffusion of Zn proceeded easily, leading to the formation of binary CuZn phases; the phases from the Cu-In system were not found. The ternary Cu-Zn-In phases were formed at temperatures of 350 and 450 °C, at which the simultaneous diffusion of In and Zn in Cu took place, with participation of liquid In and Zn. The obtained results are the starting point for the calculation of the Cu-Zn-In phase diagram which remains unavailable, in spite of fact that all Cu-Zn, In-Zn and Cu-In binary diagrams are well known.

1. Introduction

The Cu-Zn-In system is among less known systems. In spite of the well-known binary Cu-In, Cu-Zn and In-Zn phase diagrams (Ref 1-3), a ternary phase equilibrium diagram remains unknown. The reasons for that are experimental problems with the alloying of Cu, Zn and In, caused by the extreme differences in melting temperatures of the components and the possibility of intensive evaporation of Zn in the liquid state.

The interest in application of ternary Cu-Zn-In alloys concerns mainly soldering on the Au substrate or brazing processes of e.g. cast-iron, with use of the effective, mechanically strong lead free solders (Ref 4-7) with solidus and liquidus temperatures in the suitable range between 260 and 400 °C (Ref 8). Such solders would be much cheaper than the Au-based ones, and with better mechanical properties, how-

ever, their application is limited by high corrosion rates (Ref 7, 8).

To propose new soldering alloys from the Cu-Zn-In system, the phases formation and equilibria should be better known. The phase equilibria in the Cu-In Zn system were calculated on the base of thermodynamic properties of liquid alloys (Ref 7). Some vertical and isothermal sections were presented in (Ref 9). Only binary phases from the Cu-Zn and Cu-In systems were suggested (Ref 9). The present study was devoted to the determination of the formation of phases by direct diffusion at the isothermal conditions and the phase equilibria achieved in the system. The technique of diffusion multiples was chosen as the valuable experimental method, enabling the formation of all the phases which may exist in equilibrium at the specific temperature, assuming a long enough annealing time (Ref 10). The method also enables the determination of the possible diffusion paths realized by the participating metallic elements.

2. Experimental

Three types of configurations of the pure Cu, Zn and In metals in multiple joints were invented for the experiment. The isothermal annealing temperature was increased step-by–step, to preserve, as much as possible, the similar sequences of conditions for the diffusion. The annealing times and temperatures in the case of the first multiple joints configuration (S-I, Fig. 1a) were 72 hours (h) at 100 °C and 1875 h at 130 °C, the second configuration (S-II, Fig. 1b) was annealed for 72 h at 100 °C, 1875 h at 130 °C, 312 h at 300 °C, and 144 h at 350 °C (Fig. 1). The third multiple (S-III, Fig.1c) was annealing in three steps: 60 h at 130 °C, 36h at 300 °C and 336h at 450 °C (Fig. 1). The increasing temperatures caused thermally enhanced diffusion as well as increased internal pressure due to the thermal expansion of the components. The final annealing temperatures were chosen depending on the melting

Tomasz Czeppe, Anna Sypien, Anna Wierzbicka-Miernik, Grzegorz Garzeł, and **Marek Kopyto**, Institute of Metallurgy and Materials Science, Polish Academy of Sciences, Reymonta 25 St., 30-059 Krakow, Poland. Contact e-mail: t.czeppe@imim.pl.

temperatures of In and Zn components. In case of S-I joint, the highest temperature was below In melting temperature; for S-II below Zn melting temperature and for the last joint S-III the highest temperature was above Zn melting temperature. Depending on the multiplied diffusion joint configuration (Fig. 1) the pure Cu, In and Zn metals were cut into lamellas, foils or thin plates. Before the diffusion couple experiment, the surfaces of the substrates were ground with paper of 5000 maximum gradation and then cleaned with 2-propanol in an ultrasonic washer. In case of S-I system, the substrates the layers dimensions (in mm): Cu 25x9x4, Zn 13x9x3, In 11x9x3 were compressed with a steel holder. In two other cases, the components were pressed with the force of 3000 kG into Zn (S-II) or Cu (S-III) metal blocks in form of rings with external and internal dimensions ϕ20x10 and ϕ16x20, and ϕ8x8 and ϕ10 x15 (in mm), respectively. The Cu layers have the thickness of 1 mm, while before compression in the matrix soft Zn and In layers have similar thickness about 1 mm. In the case of the S-III specimen, the Cu foil of 0.2mm thickness was added to increase the ability for complete internal diffusion by Zn and In. For the layers' organization see also Fig. 1. Each system was sealed in quartz ampoule under the argon protective atmosphere and subjected to annealing in the chamber furnace. The quartz ampules with the samples were heated up, step by step, to the final annealing temperature with the heating rate of 300 °C/h. After annealing the diffusion systems were cooled down in water inside the ampule, and cut along the longitudinal axis.

The microstructure and compositions of phases were investigated on the polished cross-sections with scanning electron microscopy (SEM) FEI QUANTA 3D FEGSEM, equipped with an energy dispersion spectrometer EDS, at high vacuum (10^{-6} mbar) with the accelerating voltage 15keV. In case of the In rich phase achieved in S-I system, the melting temperature was determined with DSC Q1000 TAI. The measurements were conducted in reference to the In standard, with the heating and cooling rates of 2 and 10 K/min, using pure argon as the protective atmosphere. The experimental results were compared to the isothermal cross-section of the ternary phase diagram, calculated with the CALPHAD method based on binary approximation using PANDAT software. No ternary interactions were taken into account during calculations. Thermodynamic descriptions of binary systems come from the following references: Cu-In (Ref 11), Cu-Zn (Ref 12) and In-Zn (Ref 13).

3. Results

3.1 S-I System

The microstructures of the S-I multiple joint annealed at the solid state of all components, with the single interface between In and Zn, as well as the common interface with Cu is shown in Fig. 2. In this case, the continuous layer was formed at the Zn/Cu interface. Above the layer, the product of In infiltration along Zn grain boundaries is visible. The black points seen in the indium-rich phase (Fig. 2b) are Si fines left over from sample preparation. The results of EDS analysis at the points shown in Fig. 2 are presented in Table 1. The composition of the layer formed directly at the Cu surface and in contact with the Zn layer was determined to be $Zn_{65}Cu_{35}$ (point 2 in Fig. 2) well-fitting the γ_{CuZn} phase. The composition $In_{88}Cu_9Zn_3$ of the phase formed by the In infiltrating Zn suggests eutectic composition In-3.9 at.% Zn, known from the In-Zn binary system (Ref 3) but with some addition of Cu (point 1 in Fig. 2, Table 1). The analyses of composition revealed pure Cu and Zn in the points 3 and 4, respectively (Fig. 2, Table 1). To confirm the In-Zn eutectic, the melting temperature T_m and enthalpy of fusion ΔH_f of the infiltrating phase were determined by the DSC in relation to the In standard (Fig. 3). T_m of the phase was determined to be 143.7 °C, while the standard In melting temperature is 156.6 °C. The crystallization temperature of 142.3 °C revealed overcooling of 1.4 °C. The melting temperature agrees well with the melting temperature 143.5 °C of the In–Zn eutectic (Ref 3). Taking into account the standard enthalpy of fusion for In (28.6 J/g), for the infiltrating phase ΔH_f 33.2±0.05 J/g was determined.

3.2 S-II System

The S-II multiple joint (Fig. 1b) supplied large contacting surfaces between interlayered, relatively thick lamellas of In and Cu, surrounded by the block of Zn. Thus, the following combinations of diffusion couples were formed: In/Cu, In/Zn and Zn/Cu/In. In this case, the diffusion proceeded with the participation of the In liquid phase, while Zn and Cu remained solid. The structure of S-II joint cross-section after annealing is presented in Fig. 4. In this case, liquid In was dissolved completely infiltrating Zn, leaving voids in the volume where it was originally located as well as at the Zn. The microstructure and phase composition of the reaction products at the Zn/In
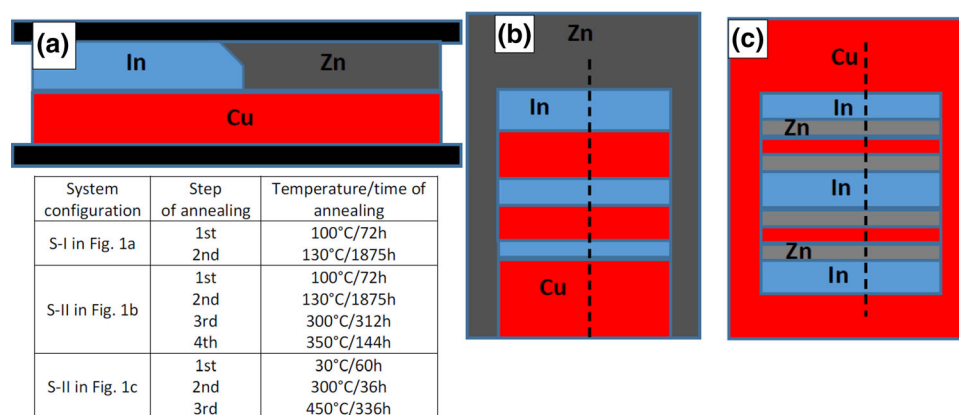

System configuration	Step of annealing	Temperature/time of annealing
S-I in Fig. 1a	1st	100°C/72h
	2nd	130°C/1875h
S-II in Fig. 1b	1st	100°C/72h
	2nd	130°C/1875h
	3rd	300°C/312h
	4th	350°C/144h
S-II in Fig. 1c	1st	30°C/60h
	2nd	300°C/36h
	3rd	450°C/336h

Fig. 1 Schematic presentation of the cross-section of three configurations of multiplied diffusion joints for the isothermal experiments: (a) S-I, (b) S-II, (c) S-III, together with the subsequent times and temperatures given in the table (Color figure online)
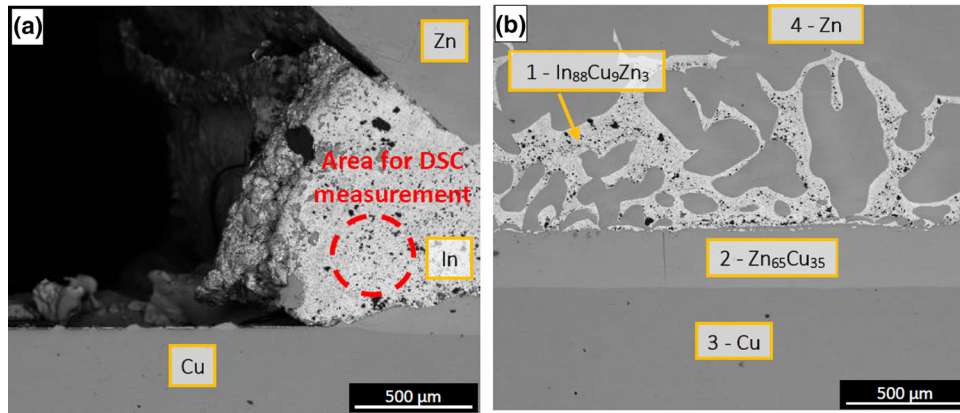
Fig. 2 The microstructure of the Cu/Zn/In diffusion triples in the S-I system: (a) Cu/Zn/In contact area, (b) joint structure in the Cu/Zn contact area with the EDS point analysis marked by numbers. The annealing steps: 100 °C/72h, 130 °C/1875h (Color figure online)

Table 1   EDS chemical composition at points 1-4 in Fig. 2

Point of analysis	In, at. %.	Cu, at. %.	Zn, at. %.	Phase identification
1	88.2	8.6	3.2	$In_{88}Cu_9Zn_3$
2	0.0	34.6	65.4	$Zn_{65}Cu_{35}$
3	0.0	100.0	0.0	Cu
4	0.0	0.0	100.0	Zn
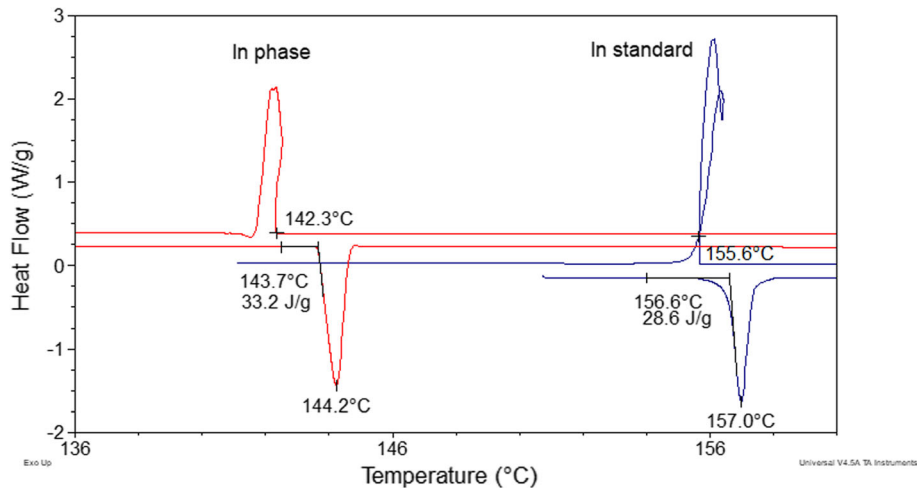
Fig. 3 DSC curves showing melting and crystallization of the In rich phase, marked by the red circle in Fig. 2a, and the In standard. Heating rate 2 K/min (Color figure online)

interface (area A in Fig. 4) which are presented in Fig. 5a, reveal Zn grain boundaries infiltrated by In in a similar way to those shown in Fig. 2.

In the area B in Fig. 4, the interlayers of two binary Cu-Zn phases were formed, at the upper and bottom interfaces of the first Cu lamella (Fig. 5b, Table 2). The Cu:Zn ratio indicates that the first layer contains the γ CuZn phase with the increased Zn content, while the second layer corresponds to the β' CuZn phase. The fact that the annealing temperature was lower than the temperature of the β phase order-disorder transition suggests that in the used experimental conditions the ordered β' phase was formed, stable up to the temperature of about 460 °C.

Lack of the participation of In in these two layers may be explained both by the ability of In to preferentially infiltrate Zn, being in contact with the In layer on the other side from Cu (Fig. 4), and by the relatively high final annealing temperature. At the bottom of the same Cu lamella (Fig. 5b, point 3), the ternary phase was formed with the composition of $Cu_{48}Zn_{40}In_{12}$ (Table 2). The same phase was detected on the upper interface in the area C (Fig. 6, point 4). The formation of the ternary phase in the case when In layer remains between two surfaces of Cu lamellas without of the possibility of rapid diffusion into Zn, indicates that In can form a phase with Cu only if the much faster diffusion of Zn into Cu occurs. For the C area, the infiltration of the CuZn phase by In was observed,

together with the precipitation of the In rich phase (Fig. 6), revealing composition corresponding to In(Cu) (Table 2, point 5 in Fig. 6). Analysis of the composition of the next discontinuous intermetallic layer (Fig. 6, point 6), indicates the formation of the β' CuZn phase from the binary system. Similar results were achieved in case of the layers formed at the surface of the bottom massive Cu (Fig. 7, Table 2), marked as D
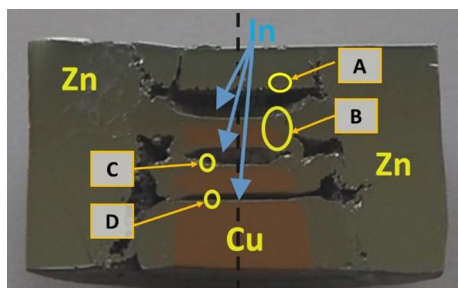

Fig. 4 Cross-section view of the S-II system joint after annealing with the In in liquid state. The places further discussed are marked by the letters. A, B, C, D showing the areas for which the interface microstructure is shown in Fig. 5, 6, 7. Final annealing 144 h at 350 °C (Color figure online)

area in Fig. 4. Except for the main surface layer, two other sublayers were noticed. The surface layer contained a homogenous phase with the composition $Cu_{49}Zn_{39}In_{12}$ infiltrated by the In rich phase (Fig. 7, Table 2), similar to the layer visible in Fig. 6. The phase of the β' CuZn composition (point 8 in Fig. 7b and Table 2), is separated from the Cu lamellae by the interlayer of Cu(Zn) solid solution (Fig. 7, Table 2, point 9), also revealing In rich precipitates. As previously, the internal volume of the Cu lamellae did not reveal any element diffused inside.

Moreover, EDS analysis revealed that the black points seen in the Fig. 7b are Si fines left from sample preparation.

3.3 S-III System

The S-III multiple join configuration (Fig. 1c) consisted of In and Zn interlayers, separated by the Cu thin foils which should be easily infiltrated by In and Zn. The whole system was surrounded by the block of Cu (Fig. 8). At the annealing temperature 450 °C both In and Zn remained liquid.

Due to the sample symmetry, the complete results were supplied by one half of the sample section marked by the rectangle in Fig. 8. The SEM micrograph, presenting localization of the sublayers of different phases above and below the Cu foil, is shown in Fig. 9. For clarity, they were marked by the numbers *l"+1" - l"+4"* and *l"-1" – l"-4"*, respectively, above
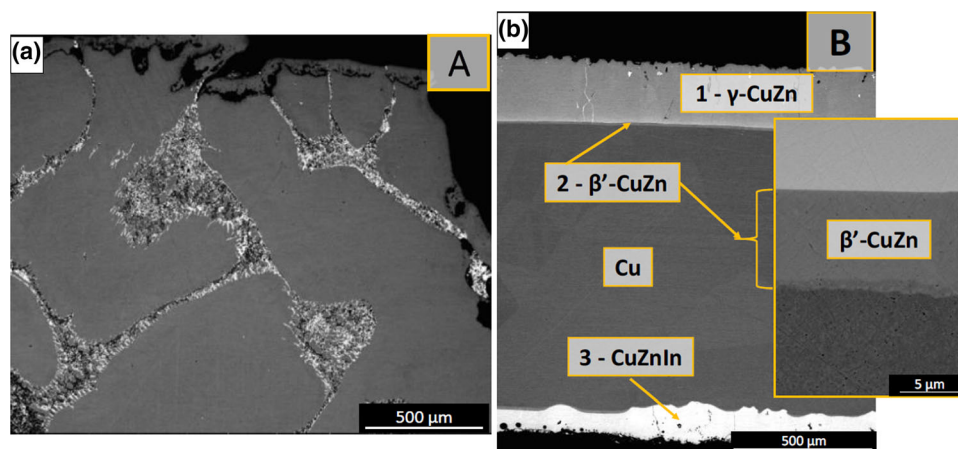

Fig. 5 The microstructure of the Cu/Zn/In diffusion triples in the S-II system formed at the: (a) Zn/In interface (area A in Fig. 4), (b) In/Cu/In interfaces of the first Cu lamella (area B in Fig. 4) with the EDS point analysis marked by numbers. Final annealing 144 h at 350 °C (Color figure online)

Table 2 EDS analysis of the composition of interlayers visible in Fig. 5b (points 1-3) Fig. 6 (points 4-6) and Fig. 7 (point 7-9)

Area marked in Fig. 4	Point of analysis (Fig. 5b, 6, 7)	Zn, at.%.	Cu, at.%.	In, at. %.	Phase identification
B	1	63.5	36.5	0	γ CuZn
	2	47.3	52.7	0	β' CuZn
	3	38.8	48.6	12.6	CuZnIn ternary phase
C	4	40.7	47.7	11.6	CuZnIn ternary phase
	5	0	9.5	90.5	In(Cu)
	6	44.6	54.2	1.2	β' CuZn
D	7	39.1	48.8	12.1	CuZnIn ternary phase
	8	45.1	53.5	1.4	β' CuZn
	9	18.7	79.8	1.5	Cu(Zn) solid solution

and below the central Cu layer (*l"0"*). Except the thin sublayers *l "±1"* formed directly at the surfaces of Cu and most external layers marked *l"±4"*, two thick layers *l"±2"* and *l" ±3"* were revealed. The microstructure of these layers *l "0" - l" ±4"*, together with the localization of the EDS analysis, are shown in
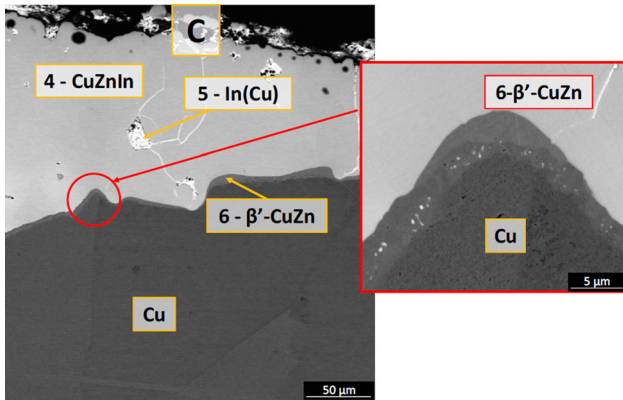

Fig. 6 The microstructure of the Cu/Zn/In diffusion triples in the S-II system formed at the top interface In/Cu of the middle Cu lamella (area C) in Fig. 4 and the *β*'- CuZn interlayer with the EDS point analysis marked by numbers. Final annealing 144 h at 350 °C (Color figure online)

Fig. 9, while the results are given in Table 3. Due to the very thin foil and relatively high temperature, the Cu layer *l"0"* contains also 2at.% of Zn (Fig. 9 Table 3, point 6). The thin *l" ±1"* interlayer of the Cu(Zn) solid solution with the composition of $Cu_{70}Zn_{30}$ was formed between Zn layer and Cu foil (Fig. 9, Table 3, points 5, 7). The next two layers, *l"±2" and l"±3"*, were formed in the localization of the original Zn lamellae with the common interface with In (Fig. 9, Table. 3, points 3, 4, 8, 9). Both revealed layers composition were near to $Cu_{50}Zn_{40}$ but with the In content in the range of 2 at.% for *l"±2"* and 7-10 at.% for *l"±3"* layers, respectively. Such large content of In in *l"±3"* may suggests formation of the metastable ternary phase. The most external layers *l"+4"* and *l"-4"* were formed in different conditions. The layer *l"+4"* formed at the interface of In and the massive Cu corps, in contact with the Zn layer, while *l"-4"* formed at the interface In/Zn foil, in the centre of the diffusion joint (Fig. 1c, 8). This interlayer reveals chemical composition of the homogeneous ternary $Cu_{55}Zn_{24}In_{21}$ matrix (Fig. 9, Table 3, points 2, 10), with precipitates rich in In (Fig. 9, Table 3, points 1, 11). In contrast to the previous cases, the replacement of In by the $Cu_{55}Zn_{24}In_{21}$ phase exhibits a mechanism of the predominant diffusion of Cu and Zn to the originally pure In layer. Concerning precipitates, the content of In between 70-90 at. % suggests formation of In eutectics or metastable In rich solid solution.
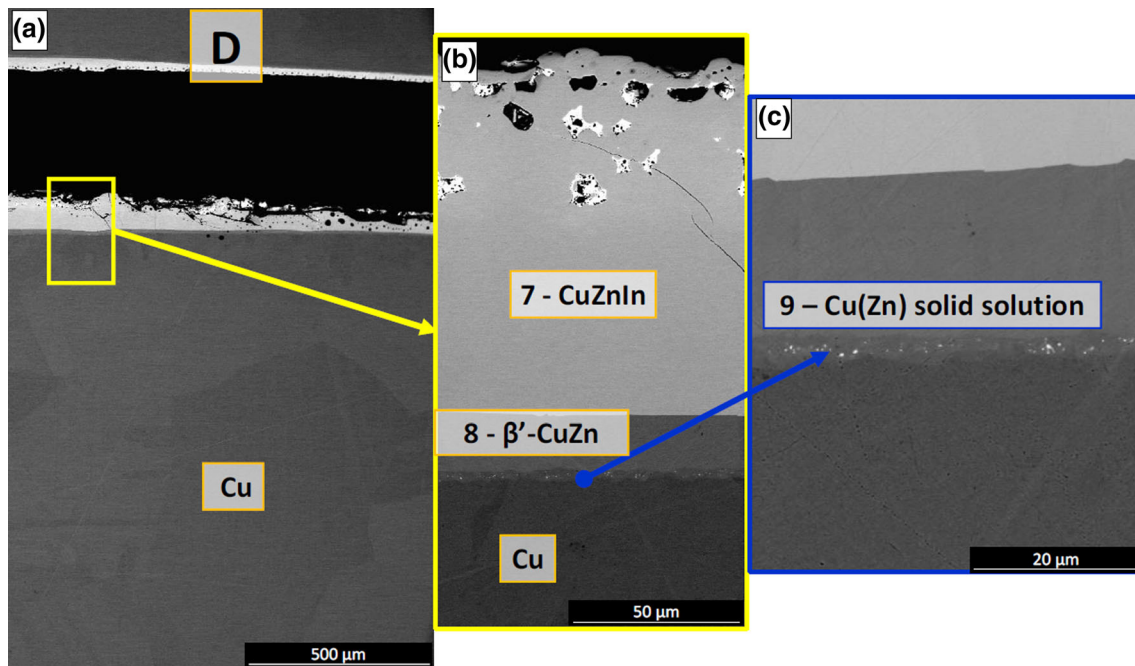

Fig. 7 The microstructure of the Cu/Zn/In diffusion triples in the S-II system of the layers formed at the: (a) Cu/InCu interface (area D in Fig. 4), (b, c) In/Cu interface being in direct contact with the In layer and side contact with the Zn surrounding block. EDS point analysis marked by numbers is shown in the figure. Final annealing 144 h at 350 °C (Color figure online)
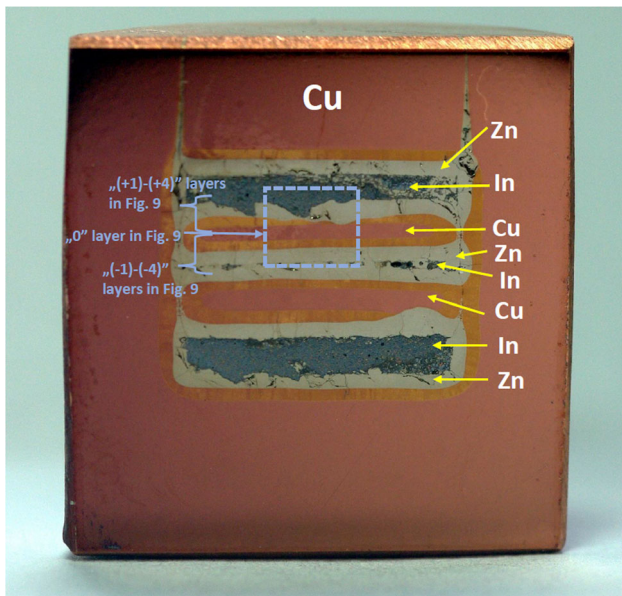
Fig. 8. Cross-section view of the S-III system joint after annealing with the In and Zn in liquid state. The yellow rectangle marked the layers further discussed. Final annealing 336h at 450 °C (Color figure online)

4. Discussion

In the case of an unknown ternary phase equilibria, especially in the range of a small additions of the third component, the basis for the analysis is the study of the range of phase fields taken from the binary systems supported by the experimental verification of a multiphase equilibria. In the presented work, the basis references were binary Cu-In (Ref 11), Cu-Zn (Ref 12) and In-Zn (Ref 13) systems used to model the ternary phase diagram in Fig. 10 with the CALPHAD method. Calculations of isothermal cross-sections of the ternary Cu-In-Zn system were carried out by extrapolation from thermodynamic descriptions of binary systems (Ref 11–13) without taking ternary interactions into account. The results reveal some specific ability of metallic elements In, Zn and Cu for the diffusion and phase formation during interaction at increased temperatures. As results, In can very easily diffuse along the Zn grain boundaries below its melting temperature, forming In(Zn)-Zn eutectic phase, however, it does not diffuse into Cu. On the other hand, at a such low temperature Zn and Cu formed γ CuZn phase at the interface. The In behaviour, infiltrating Zn along the interfaces both in solid and liquid state finds support in results presented in (Ref 14); showing that due to the positive deviation from the ideal In-Zn solution in the liquid state and high surface tension of liquid In, the surface layer of In-Zn alloys remains greatly enriched in In proportionally to its content.

At temperature of annealing higher then melting temperature, In intensively infiltrated both Zn grain boundaries and CuZn phases. Neither diffusion of Zn nor In into Cu volume was noticed but the layers of γ and β' CuZn phases formed in the case of some scarcity of In. In, if available preferentially, infiltrated Zn and formed ternary CuZnIn phases. The composition of CuZn phases seems clearly related to the diffusion distance from the Zn interface. The γ CuZn phase, enriched in Zn, formed at the Zn interface while β'CuZn phase formed directly at the interface of Cu. At the longest distances required for the Zn diffusion, Cu(Zn) solid solution but not CuZn phases formed at the interfaces. The phase compositions are presented in Fig. 10. The last case, concerning diffusion of In and Zn if both are in a liquid state, supports the conclusion that In may easy diffuse into Cu only in the presence of the simultaneous diffusion of Zn. In this case, the Cu foil was separated from In by the Zn layer. As a result, the sequence of ternary phases was formed with the Cu:Zn proportions adequate for Cu(Zn) solid solution enriched with In, its content decreasing from 20 to 2 at.%. The nature and sequence of the phases formed appeared to be symmetric with respect to each Cu layer. This indicates that Cu is a barrier for the In diffusion, in contrast to the simultaneous diffusion of Cu and In into the Zn, leading to the formation of ternary phases. The identification of the ternary phases by the SEM/EDS composition analysis allowed for the modelling of the hypothetical cross-section of the phase diagram using the PANDAT program by the extension of equilibria from the binary systems (Fig. 10).

5. Conclusions

1. Below melting temperature In reveals preferential ability for the diffusion in Zn along the grain boundaries forming the In-Zn eutectic phase.
2. Ternary phases were formed by diffusion in the annealing procedures by 144 and 336 hours at temperatures 350 and 450 °C, respectively.
3. In all applied temperatures pure Cu revealed to be the barrier for the diffusion of In while Zn diffusion proceeded easily leading to the formation of binary phases belonging to the Cu-Zn system, including the Zn rich γ phase.
4. At higher temperatures, at which the simultaneous diffusion of In and Zn in Cu or In and Cu in Zn took place, with participation of the liquid In and Zn, the ternary phases formed, with the content of In up to 20 at.% and the proportion of Cu:Zn adequate to the phases formed in the binary Cu-Zn system, from the Cu solid solution to the CuZn γ phase, with Zn content up to 67 at.%.
5. In the applied experimental conditions the phases belonging to the Cu-In system were not formed.
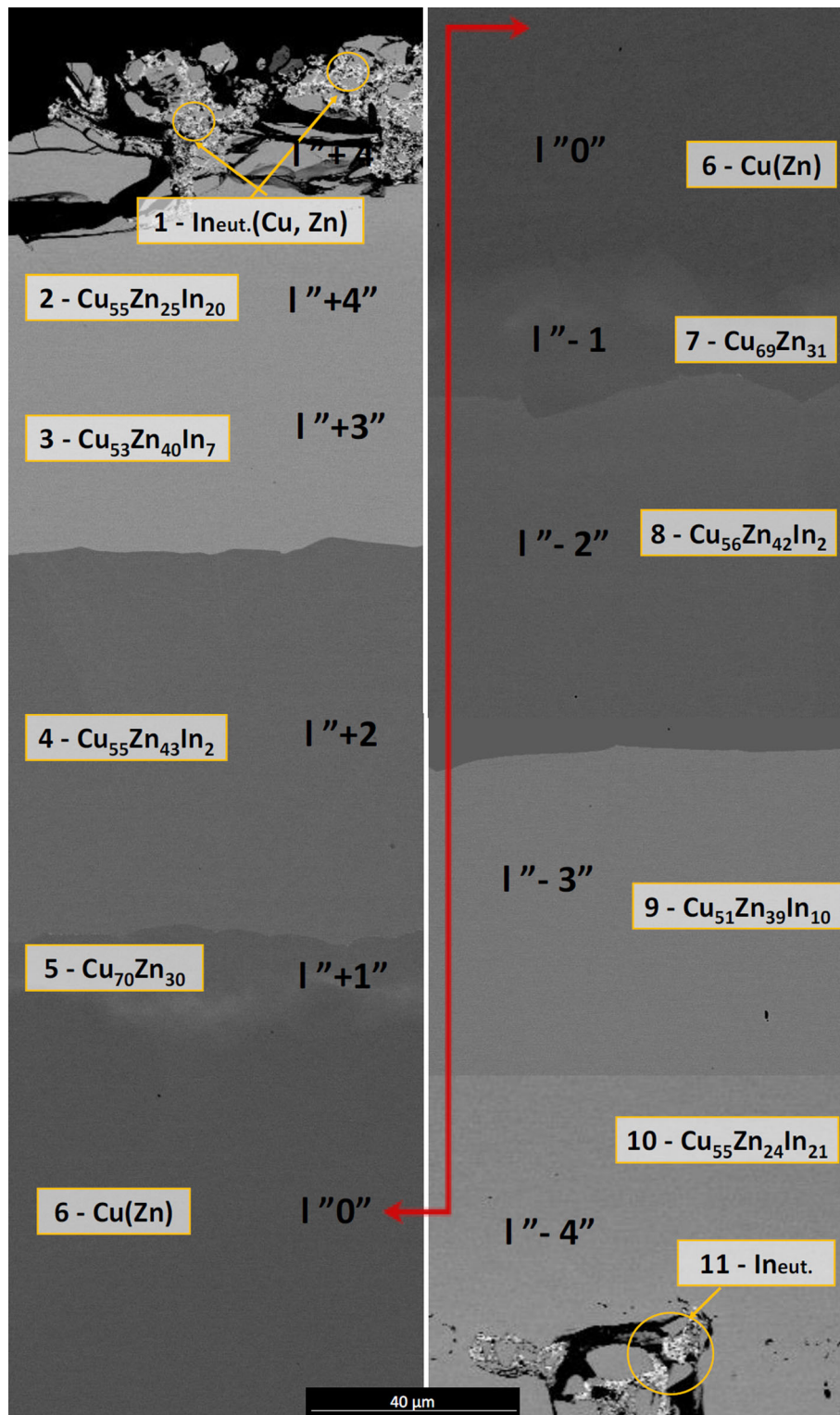
Fig. 9. Microstructure of the symmetrical sequence of layers formed in the S-III system analyzed in the areas marked in Fig. 8: (a) layers l"+4" – "0", (b) layers l"0" - "−4". Results of the EDS point analysis at points 1-11 are given in Table 3. Final annealing 336h at 450 °C (Color figure online)

Table 3 EDS analysis of the composition of layers and interlayers visible in Fig. 9

Number of the layer	Point of analysis (Fig. 9)	Zn, at.%.	Cu, at.%.	In, at.%.	Phase identification
l"+4"	1	6.5	7.7	85.3	In(Cu,Zn)
	2	25.0	54.8	20.2	CuZnIn ternary phase
l"+3"	3	40.0	52.9	7.1	CuZnIn ternary phase
l"+2"	4	42.5	56.0	1.5	Cu(In)Zn phase
l"+1"	5	29.7	70.3	0.0	Cu(Zn) solid solution
l"-0"	6	2.2	97.8	0.0	Cu
l"-1"	7	31.0	69.0	0.0	Cu(Zn) solid solution
l"-2"	8	42.5	55.9	1.7	Cu(In)Zn phase
l"-3"	9	38.7	51.2	10.1	CuZnIn ternary phase
l"-4"	10	23.7	55.3	21.0	CuZnIn ternary phase
	11	7.5	15.4	77.1	In(Cu,Zn)
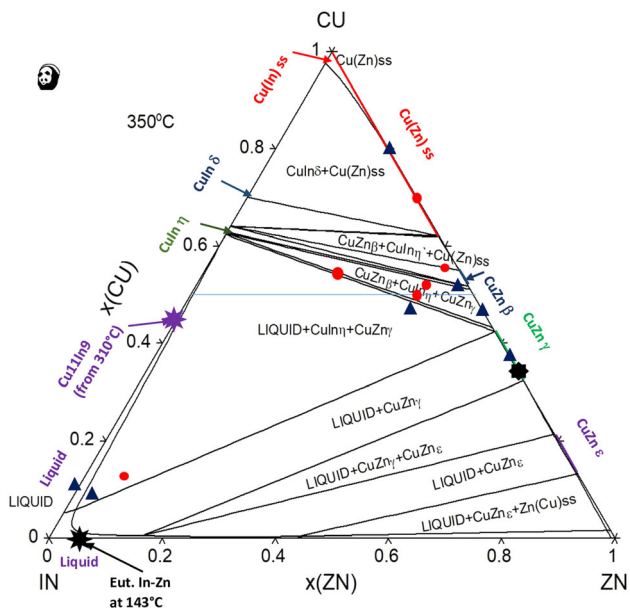
Fig. 10. Isothermal section of the hypothetical Cu-Zn-In phase equilibrium diagram at 350 °C modelled by the binary equilibria extension with use of the CALPAD strategy with marked compositions of the detected phases, binary and ternary: Black Asterisk phases formed in the S-I system (projection from 130 °C), Blue Triangle phases formed in the S-II system, and Red Circle phases formed in S-III system (projection from 450 °C) (Color figure online)

References

1. P.R. Subramanian and D.E. Laughlin, Cu-In Phase Diagram, *Bin. Alloys Phase Diagr.*, 1989, **10**, p 1425.
2. A.P. Miodownik, Cu-Zn Phase Diagram, *Bin. Alloys Phase Diagr.*, 1989, p. 1509
3. J. Dutkiewicz and W. Zakulski, In-Zn Phase Diagram, *Bin. Alloys Phase Diagr.*, 1984, p. 2318
4. A. Dinsdale et al., Atlas of phase diagrams for Lead Free Solders COST 531 Lead Free Soldering, Vol.1 p 82
5. A. Dinsdale et al., Atlas of phase diagrams for Lead Free Solders COST 531 Lead Free Soldering Vol.1 p. 115
6. J.-E. Lee, K.-S. Kim and K. Suganuma, Mauhiro Inoue and Goro Izuta Thermal Properties and Phase Stability of Zn- Sn and Zn-In Alloys as High Temperature Lead-Free Solder, *Mat. Trans.*, 2007, **48**, p 584–593.
7. C.-J. Sabine Knott, Chen, Friedrich Gehringer, Adolf Mikula, Thermodynamic Properties of Liquid Cu-In-Zn Alloys, *Int. J. Mat. Res.*, 2006, **97**(8), p 1102–1107.
8. B. Kim, C.-W. Lee, D. Lee and N. Kang, Effect of Sb Addition on Bi-26Ag-01Cu Solders for High-Temperature Applications, *J. Alloys Comp.*, 2014, **592**, p 207–212.
9. V.P. Vassiliev and V.A. Lysenko, Thermodynamic Evolution of the Cu-In-Zn System, *Lett./J. Alloys Compounds*, 2016, **681**, p 606–612.
10. J.C. Zhao, The Role of Phase Transformation Kinetics in Phase Diagram Determination and Assessment, *Methods Phase Diagr. Determ.*, 2007 https://doi.org/10.1016/b978-008044629-5/50002-1
11. H.S. Liu, Y. Cui, K. Ishida et al., Thermodynamic Assessment of the Cu-In Binary System, *JPE*, 2002, **23**, p 409. https://doi.org/10.1361/105497102770331352
12. M. Kowalski and P.J. Spencer, Thermodynamic Reevaluation of the Cu-Zn System, *JPE*, 1993, **14**, p 432–438. https://doi.org/10.1007/BF02671961
13. B.J. Lee, Thermodynamic Assessments of the Sn-Zn and In-Zn Binary Systems, *Calphad*, 1996, **20**, p 471–480. https://doi.org/10.1016/S0364-5916(97)00009-6
14. J. Pstrus, Z. Moser and W. Gasior, Surface Properties of Liquid In-Zn Alloys, *Appl. Surf. Sci.*, 2011, **257**, p 3867–3871.